

Activation mechanism of ammonium oxalate with pyrite in the lime system and its response to flotation separation of pyrite from arsenopyrite

Runpeng Liao, Shuming Wen, Qicheng Feng, Jiushuai Deng, and Hao Lai

Cite this article as:

Runpeng Liao, Shuming Wen, Qicheng Feng, Jiushuai Deng, and Hao Lai, Activation mechanism of ammonium oxalate with pyrite in the lime system and its response to flotation separation of pyrite from arsenopyrite, *Int. J. Miner. Metall. Mater.*, 30(2023), No. 2, pp. 271-282. <https://doi.org/10.1007/s12613-022-2505-5>

View the article online at [SpringerLink](#) or [IJMMM Webpage](#).

Articles you may be interested in

Hong Qin, Xue-yi Guo, Qing-hua Tian, and Lei Zhang, [Recovery of gold from refractory gold ores: Effect of pyrite on the stability of the thiourea leaching system](#), *Int. J. Miner. Metall. Mater.*, 28(2021), No. 6, pp. 956-964. <https://doi.org/10.1007/s12613-020-2142-9>

Zhen Xue, Zhen-yuan Nie, Hong-chang Liu, Wei-bo Ling, Qian Pan, Jin-lan Xia, Lei Zheng, Chen-yan Ma, and Yi-dong Zhao, [Effect of the surface microstructure of arsenopyrite on the attachment of *Sulfobacillus thermosulfidooxidans* in the presence of dissolved As\(\)](#), *Int. J. Miner. Metall. Mater.*, 28(2021), No. 7, pp. 1135-1144. <https://doi.org/10.1007/s12613-020-2231-9>

Jin-sheng Yu, Run-qing Liu, Li Wang, Wei Sun, Hong Peng, and Yue-hua Hu, [Selective depression mechanism of ferric chromium lignin sulfonate for chalcopyrite–galena flotation separation](#), *Int. J. Miner. Metall. Mater.*, 25(2018), No. 5, pp. 489-497. <https://doi.org/10.1007/s12613-018-1595-6>

Ri-jin Cheng, Hong-wei Ni, Hua Zhang, Xiao-kun Zhang, and Si-cheng Bai, [Mechanism research on arsenic removal from arsenopyrite ore during a sintering process](#), *Int. J. Miner. Metall. Mater.*, 24(2017), No. 4, pp. 353-359. <https://doi.org/10.1007/s12613-017-1414-5>

Xiong Chen, Guo-hua Gu, Li-juan Li, and Ren-feng Zhu, [The selective effect of food-grade guar gum on chalcopyrite-monoclinic pyrrhotite separation using mixed aerofloat \(CSU11\) as collector](#), *Int. J. Miner. Metall. Mater.*, 25(2018), No. 10, pp. 1123-1131. <https://doi.org/10.1007/s12613-018-1663-y>

Xiong Chen, Guo-hua Gu, and Zhi-xiang Chen, [Seaweed glue as a novel polymer depressant for the selective separation of chalcopyrite and galena](#), *Int. J. Miner. Metall. Mater.*, 26(2019), No. 12, pp. 1495-1503. <https://doi.org/10.1007/s12613-019-1848-z>





IJMMM WeChat



QQ author group

Activation mechanism of ammonium oxalate with pyrite in the lime system and its response to flotation separation of pyrite from arsenopyrite

Runpeng Liao^{1,2}, Shuming Wen^{1,2}, Qicheng Feng^{1,2},, Jiushuai Deng^{3,4},, and Hao Lai^{1,2}

1) State Key Laboratory of Complex Nonferrous Metal Resources Clean Utilization, Faculty of Land Resource Engineering, Kunming University of Science and Technology, Kunming 650093, China

2) Yunnan Key Laboratory of Green Separation and Enrichment of Strategic Mineral Resources, Kunming University of Science and Technology, Kunming 650093, China

3) School of Chemical & Environmental Engineering, China University of Mining & Technology (Beijing), Beijing 100083, China

4) Liuzhou China-Tin Nonferrous Design and Research Institute Co., Ltd., China Tin Group, Liuzhou 545006, China

(Received: 15 March 2022; revised: 18 April 2022; accepted: 19 April 2022)

Abstract: The activation properties of ammonium oxalate on the flotation of pyrite and arsenopyrite in the lime system were studied in this work. Single mineral flotation tests showed that the ammonium oxalate strongly activated pyrite in high alkalinity and high Ca^{2+} system, whereas arsenopyrite was almost unaffected. In mineral mixtures tests, the recovery difference between pyrite and arsenopyrite after adding ammonium oxalate is more than 85%. After ammonium oxalate and ethyl xanthate treatment, the hydrophobicity of pyrite increased significantly, and the contact angle increased from 66.62° to 75.15° and then to 81.21° . After ammonium oxalate treatment, the amount of ethyl xanthate adsorption on the pyrite surface significantly increased and was much greater than that on the arsenopyrite surface. Zeta potential measurements showed that after activation by ammonium oxalate, there was a shift in the zeta potential of pyrite to more negative values by adding xanthate. X-ray photoelectron spectroscopy test showed that after ammonium oxalate treatment, the O 1s content on the surface of pyrite decreased from 44.03% to 26.18%, and the S 2p content increased from 14.01% to 27.26%, which confirmed that the ammonium oxalate-treated pyrite surface was more hydrophobic than the untreated surface. Therefore, ammonium oxalate may be used as a selective activator of pyrite in the lime system, which achieves an efficient flotation separation of S–As sulfide ores under high alkalinity and high Ca^{2+} concentration conditions.


Keywords: pyrite; arsenopyrite; ammonium oxalate; flotation separation

1. Introduction

Pyrite (FeS_2) is the most widely distributed sulfide mineral, often associated with metal sulfide minerals such as lead, zinc, and copper [1–2]. Arsenic-bearing sulfide minerals such as arsenopyrite (FeAsS) are usually associated with pyrite in metal sulfide minerals [3]. Froth flotation is the most widely used and most effective method for the mineral processing of metal sulfide minerals. In order to enhance the difference of mineral surface characteristics of polymetallic sulfide ores and effectively separate each objective minerals, many collectors, modifiers, depressants, or frothers are used for mineral flotation separation. Lime (in the form of CaO , or $\text{Ca}(\text{OH})_2$) has been widely used as a depressant of pyrite and arsenopyrite in polymetallic sulphide ores flotation because of its wide range of sources, low price, and high efficiency [4–5]. The flotation separation of pyrite and arsenopyrite in high alkalinity and high Ca^{2+} ion concentration pulp is the most representative, typical, and difficult in separating complex polymetallic sulfide ores. The effective separation of

pyrite and arsenopyrite helps to make full use of S and Fe resources in pyrite and avoid the harm of arsenic to the subsequent smelting and processing of pyrite concentrate [6].

The surface adsorption, oxidation, and floatability of pyrite and arsenopyrite in a high-alkaline lime system are very resemble. There are hydrophilic components such as CaO , CaSO_4 , $\text{Ca}(\text{OH})_2$, and $\text{Fe}(\text{OH})_3$ on the surface of pyrite or arsenopyrite by lime as depressant [7–8]. In order to separate pyrite and arsenopyrite minerals from the lime system, activators are usually used to moderately activate pyrite and arsenopyrite in flotation [8]. Sulfuric acid is the most widely used activator for the flotation of pyrite and arsenopyrite in the lime system. However, sulfuric acid consumption is large, the selectivity of activation is low, and the dilution of concentrated sulfuric acid is inconvenient. The reaction between sulfuric acid and pyrite in pulp will dilute and release highly toxic hydrogen sulfide gas, deteriorate the production and operation environment, and there are great potential safety hazards [9]. The tailings treated with sulfuric acid will also produce a large amount of acid wastewater, ser-

 Corresponding authors: Qicheng Feng E-mail: fqckmust@163.com; Jiushuai Deng E-mail: dengshuai689@163.com

© University of Science and Technology Beijing 2023

iously damaging the ecological environment [10]. Therefore, it is necessary to study the selective activation of pyrite under alkaline conditions.

Ammonium salts have been studied as activators for a long time. It has been found that ammonium salts such as NH_4NO_3 , $(\text{NH}_4)_2\text{SO}_4$, NH_4F , $(\text{NH}_4)_2\text{CO}_3$, and NH_4Cl can improve the recovery of pyrite [11–12]. Some concentrators have adopted ammonium sulfate and ammonium bicarbonate to activate pyrite in lime pulp systems. Ammonium salt can activate pyrite in high alkaline and high Ca^{2+} concentration pulp, mainly because ammonium salt can appropriately decrease the pH value of pulp, dissociate the hydrophilic oxide film on the mineral surface, and catalyze the formation of double xanthate. However, there are few studies on the selectivity of pyrite and arsenopyrite in the process of ammonium salt activation.

Ammonium oxalate $(\text{NH}_4)_2\text{C}_2\text{O}_4$ is prepared by the reaction of ammonia and oxalic acid. It is cheap, has a wide range of sources, and is non-toxic and harmless. Oxalate ions have a stronger ability to complexation with calcium ions than sulfate and carbonate. In the high alkaline and high calcium concentration pulp system, the difference of physical and chemical properties between pyrite and arsenopyrite is greater than the original difference of surface properties between pyrite and arsenopyrite. This makes it possible for ammonium oxalate to activate pyrite from arsenopyrite selectively.

In this work, micro-flotation tests and open circuit verification tests of actual ore were performed to separate pyrite from arsenopyrite using ammonium oxalate as a selective activator in a high-alkaline lime system. The interaction mechanism between ammonium oxalate and pyrite in the lime sys-

tem was investigated through contact angle measurements, surface adsorption experiments, zeta potential measurements, and X-ray photoelectron spectroscopy (XPS) studies.

2. Experimental

2.1. Materials

Pyrite and arsenopyrite with high purity were obtained from Yunnan province, China. High-grade and appropriate pyrite and arsenopyrite specimen sizes were acquired by manual selection, crushed, dry ground, and dry screened. The particle size of $-75+45\ \mu\text{m}$ was used for flotation tests, surface-adsorption measurements, and XPS measurements. A minerals sample ($<5\ \mu\text{m}$) was used for zeta potential measurements. The polished lump ore was used for the contact angle measurement. Moreover, an As-bearing pyrite tailings (China Tin Mining Co., Ltd.) containing 27.48wt% sulfur and 2.07wt% arsenic was used in the open circuit verification test. Fig. 1 shows the X-ray diffraction (XRD) phase analysis of the pure pyrite and arsenopyrite by using the MDI Jade 6.0 Package. The chemical multi-element analysis results of both pyrite and arsenopyrite are listed in Table 1. It is seen that there are only minute quantity gangue minerals in both samples, which can be used for pure mineral flotation and mechanism investigation.

Analytically pure ammonium oxalate was employed as an activator. Analytically pure lime was used as a pH adjuster and depressant. Potassium ethyl xanthate (PEX) and pine oil, which was of industrial purity, were used as collector and frother. In addition, pure deionized water with a resistivity of $18.3\ \text{M}\Omega\cdot\text{cm}$ was used in all experiments.

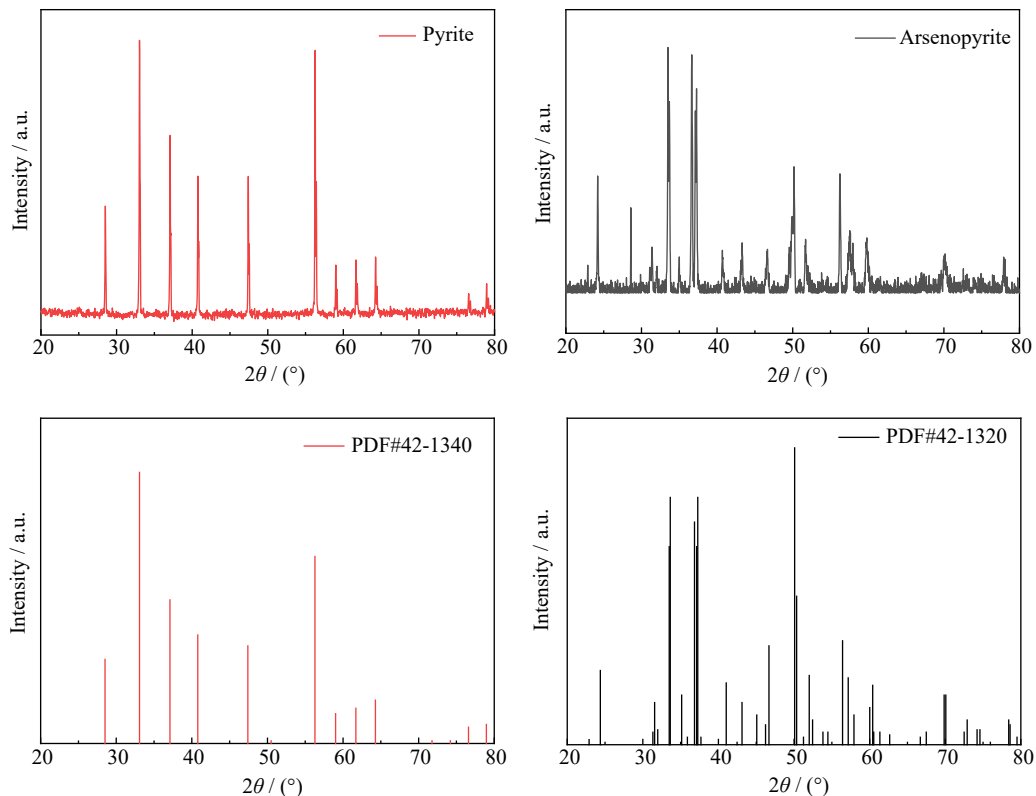


Fig. 1. XRD patterns of the purified pyrite and arsenopyrite and their standard PDF cards.

Table 1. Multi-element analyses of pyrite and arsenopyrite

wt%

Components	Fe	S	As	SiO ₂	MgO	CaO	Al ₂ O ₃
Pyrite	46.04	52.44	—	0.52	0.21	0.45	0.23
Arsenopyrite	34.16	19.05	45.18	0.79	0.05	0.06	0.13

2.2. Flotation tests

2.2.1. Micro-flotation tests

An RK/FGC 5-35 trough-type flotation machine was used for micro-flotation tests. In the micro-flotation tests, 2 g of pure mineral samples were treated with an ultrasonic cleaner for 5 min to remove the oxidized components from the mineral surface, and the supernatant was removed. The mineral sample was mixed with 30 mL deionized water and added to

the flotation cell at 1600 r/min. The pulp’s pH was measured by a pH meter (PHS-3C, Wincom, China). Fig. 2(a) shows that after ultrasonic cleaning and flotation machine stirring for 1min, add lime, ammonium oxalate (if need), PEX, and pine oil to the pulp in sequence. After 3 min of flotation, the floating and sunken materials were collected and dried, then the recovery was calculated from the weight of the dried products. Three tests were repeated, and the average was obtained.

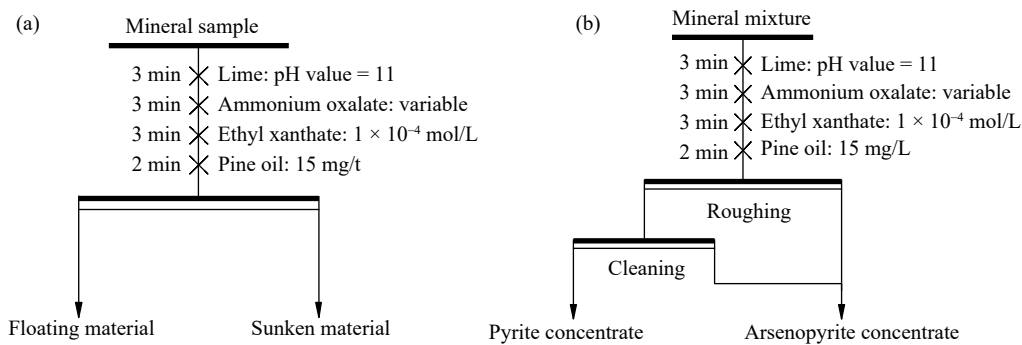


Fig. 2. Flowsheet of the micro-flotation test for (a) a single mineral and (b) the mineral mixture.

Mixed pyrite–arsenopyrite flotation separation tests were carried out to verify the selective activation performance of ammonium oxalate in the lime system. As shown in Fig. 2(b), the flotation reagent system of the mineral mixture (1 g pyrite and 1 g arsenopyrite) flotation was consistent with the single-mineral flotation. The flotation recovery of pyrite and arsenopyrite is calculated by the yield and element grade of the froth and sink products. The flotation recovery of pyrite and arsenopyrite recovery was calculated from chemical assays of the sulfur and arsenic of the concentrate and tailings.

2.2.2. Actual ore flotation tests

An open-circuit ore flotation test was conducted on an XFG-0.5 L single-trough flotation machine to verify whether the ammonium oxalate can be used as a selective activator in industrial production. Fig. 3 shows the flowsheet of the open-circuit ore flotation test. After the test, the recovery was calculated by the product grades assessed by the chemical analysis. The As-bearing pyrite tailings were produced from the previous flotation separation of cassiterite, galena, and sphalerite.

2.3. Contact angle measurements

The contact angle can characterize the surface wettability of pyrite and arsenopyrite. The massive mineral was cut into a cube (1.0 cm × 1.0 cm × 0.2 cm) and polished. For polished pyrite and arsenopyrite, the following test steps were continuously carried out: (1) the polished pyrite and arsenopyrite samples were soaked in alkaline lime solution at pH value of 11 for 3 min; (2) add 4 × 10⁻³ mol/L ammonium oxalate to the lime solution system and reacted for 3 min; (3) finally, add 1 × 10⁻⁴ mol/L PEX for 3 min. JY-82B video con-

tact angle tester was used to measure the contact angles of deionized water drops on the surface of pyrite and arsenopyrite under different treatment conditions. Then the shape of the deionized water drops under different treatment conditions was photographed by the CCD camera system, and the contact angle values were obtained by measuring the angle or height. Repeat the measurement three times for each test, and calculate its average value and standard deviation.

2.4. Adsorption capacity test

In this experiment, the concentration of PEX in pulp with different ammonium oxalate concentration treatments was determined by ultraviolet–visible spectrophotometer, then the

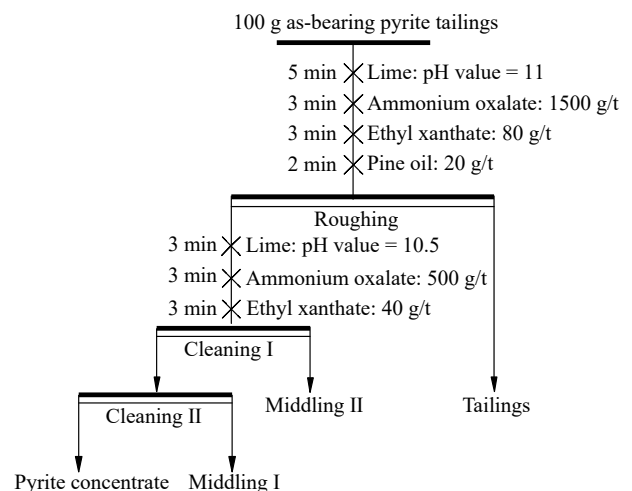


Fig. 3. Flowsheet of the actual ore flotation.

adsorption concentration of PEX on pyrite and arsenopyrite can be calculated. Approximately 2 g of samples were taken each time for adsorption experiments. Firstly, the mineral was cleaned by ultrasound and mixed with 30 mL deionized water on the magnetic stirrer. Then the pulp was adjusted to pH value of 11 with lime. After that, different concentrations of ammonium oxalate and 1×10^{-4} mol/L PEX were added to the pulp successively and acted for 3 min. Finally, the mixture was filtered and centrifuged, and 5 mL of supernatant was taken for testing. Each experiment was repeated three times to calculate the average values and the standard deviations.

The calculation formula of adsorption capacity was described as following:

$$\Gamma_M = \frac{(C_0 - C)V}{m} \quad (1)$$

where Γ_M is the adsorption concentration of ethyl xanthate (mol/g), C_0 is the initial concentration of ethyl xanthate in pulp (mol/L), C is the residual concentration of ethyl xanthate in pulp (mol/L), V is the volume of pulp (L), and m is the mass of mineral (g).

2.5. Zeta potential measurements

The zeta potential of the pyrite and arsenopyrite samples was measured by a Zetasizer Nano Zs 90 (Malvern Instruments Co., Malvern, UK). The purified mineral particles were ground in an agate planetary ball mill until the particle size was less than 5 μm , weighed 20 mg each time, and put in a 40 mL electrolyte solution containing 1×10^{-3} mol/L potassium chloride. A magnetic stirrer dispersed the mineral particles in the pulp, and the pulp was adjusted according to the same agent dosage as the flotation test. Adjust the pulp pH with the supernatant of limewater, then the pulp was settled for 5 min, and the supernatant of the refined particle suspension was used for zeta potential measurement. Zeta potential was measured three times, and the average value and standard deviation were calculated as the final result.

2.6. XPS analysis

The X-ray photoelectron spectroscopy was recorded using a scanning XPS microprobe system (PHI 5000 Versa Probe II, ULVAC-PHI, Japan). The chemical composition and the concentration variation of element content on the pyrite and arsenopyrite surface before and after interaction with 4×10^{-3} mol/L ammonium oxalate in lime solution at pH value of 11 were measured. The pulp was stirred in a magnetic stirrer according to the surface adsorption experiments. The powder samples were filtered and separated, then put into the vacuum drying oven for drying. The dried sample was subjected to 200 W monochromatic Al K_{α} radiation (1486.7 eV). First, the XPS took comprehensive survey scans and detailed scans of the C 1s, O 1s, Fe 2p, S 2p, and As 3d (only arsenopyrite samples) regions. The MultiPak software processed the measured data, and the spectrum was calibrated concerning the C 1s peak at 284.8 eV. The narrow-scan spectra of the samples were fitted via the Gauss–Lorentz method.

3. Results and discussion

3.1. Flotation tests

3.1.1. Single mineral flotation

Fig. 4 shows the variation of pyrite and arsenopyrite flotation recovery as a function of ammonium oxalate concentration in the lime system at pH value of 11 and an ethyl xanthate's concentration of 1×10^{-4} mol/L. Without the addition of ammonium oxalate, the flotation recovery of pyrite and arsenopyrite was lower than 10% by lime as depressant. Low recoveries of both pyrite and arsenopyrite were obtained using lime as depressant and pH adjuster, indicating that both minerals have poor floatability after adding lime. When the concentration of ammonium oxalate increased from 0 to 4×10^{-3} mol/L, the recovery of pyrite obviously increased from 6.32% to 87.29%, while that of arsenopyrite was only mildly affected. At the same time, the pulp pH was always maintained at low alkalinity conditions. When the concentration of ammonium oxalate was higher than 4×10^{-3} mol/L, the recovery of arsenopyrite showed an upward trend, indicating that ammonium oxalate will also slightly activate arsenopyrite at high concentration. Thus, it was concluded that adding ammonium oxalate could significantly increase the ethyl xanthate-induced flotation differences of pyrite and arsenopyrite in the lime system. This is explained that pyrite is more easily activated under the same conditions.

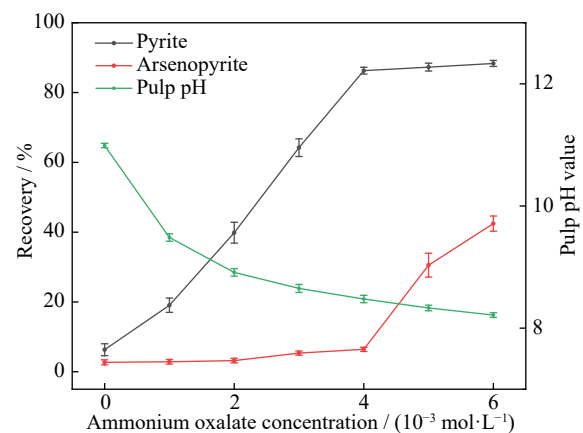


Fig. 4. Flotation recovery and pulp pH of pyrite and arsenopyrite in the lime system as a function of the ammonium oxalate concentration.

3.1.2. Mineral mixture flotation tests

In order to verify the selective activation of ammonium oxalate on pyrite, the flotation separation test of the pyrite–arsenopyrite mixture was carried out. According to single mineral flotation results, three different concentrations of ammonium oxalate were selected for the separation test of the mineral mixture. The yield, grade, and flotation recovery of S concentrate and As concentrate in the mineral mixture system are shown in Table 2. When the concentration of ammonium oxalate increased from 3 to 5×10^{-3} mol/L, the recovery of pyrite in S concentrate increased from 86.86% to 91.80%. In comparison, the recovery of arsenopyrite in S concentrate only increased from 3.74% to 10.74%, and the

Table 2. Selective flotation results for the mixture of pyrite and arsenopyrite

(NH ₄) ₂ C ₂ O ₄ concentration / (10 ⁻³ mol·L ⁻¹)	Products	Yield / %	Grade / wt%		Recovery / %	
			S	As	FeS ₂	FeAsS
3	S Concentrate	45.30	47.38	1.86	86.86	3.74
	As Concentrate	54.70	25.24	39.67	13.14	96.26
4	S Concentrate	47.64	47.43	2.21	90.61	4.67
	As Concentrate	52.36	24.21	41.03	9.39	95.33
5	S Concentrate	51.27	46.80	4.72	91.80	10.74
	As Concentrate	48.73	23.14	41.29	8.20	89.26

floatability of arsenopyrite remains at a very low level. The separation test results of the mineral mixture showed that ammonium oxalate could selectively activate pyrite. The difference in flotation recovery is more than 85% under the optimum conditions. Therefore, ammonium oxalate could be an effective pyrite activator in the flotation separation of pyrite from arsenopyrite under a high alkalinity system.

3.1.3. Actual ore flotation tests

The flotation separation test of as-bearing pyrite tailings was carried out with ammonium oxalate as an activator. After open-circuit flotation (Table 3), the pyrite concentrate produced contains 53.46wt% S and 0.61wt% As, indicating that the recovery of S in pyrite concentrate is 63.97%, and that of As is 9.70%. Meanwhile, the tailings contained 8.40wt% S and 2.86wt% As, suggesting a recovery of 69.65% As in tailings. The results indicated that an effective separation of pyrite and arsenopyrite could be achieved with ammonium oxalate as an activator.

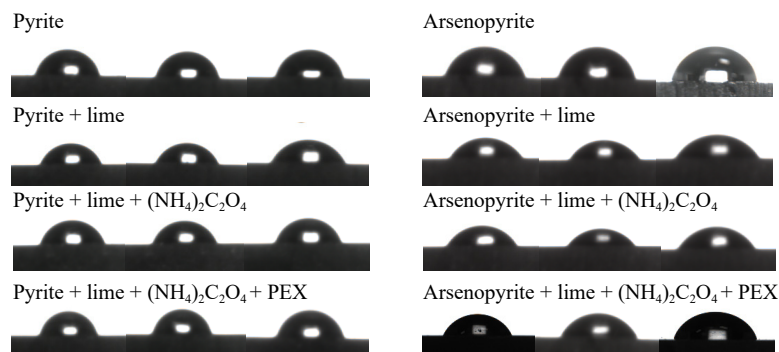
3.2. Contact angle analysis

The contact angle can directly reflect the wettability of the mineral surface [13–14]. In order to investigate the activation characteristics of ammonium oxalate, the contact angle of pyrite and arsenopyrite under different chemical treatment

conditions were measured, and the results are presented in Figs. 5 and 6. The contact angles of the polished pyrite and arsenopyrite were 79.33° and 77.31°, respectively. It shows that pyrite and arsenopyrite have natural hydrophobicity. Then adding samples in alkaline lime solution at pH value of 11 for 5 min, the contact angles of pyrite and arsenopyrite decreased by 12.71° and 17.15°, respectively. This change indicated that both pyrite and arsenopyrite formed hydrophilic surfaces under the highly alkaline lime system. After adding ammonium oxalate, the contact angle of pyrite increased by 12.33°, while that of arsenopyrite decreased by 0.64°. The results show that adding ammonium oxalate can clean the hydrophilic film on the surface of pyrite treated by lime to change the pyrite surface's wettability significantly, but has no significant effect on arsenopyrite. Finally, with a further introduction of PEX, the contact angle of pyrite increased from 75.15° to 81.21°, and the contact angle of arsenopyrite only increased from 59.52° to 62.41°. This result indicates that xanthate can be effectively adsorbed on the surface of pyrite after activation by ammonium oxalate. The difference in contact angle between pyrite and arsenopyrite reached 19.80° in the flotation system, indicating that pyrite can be effectively separated from arsenopyrite.

Table 3. Result of the open-circuit flotation

Product	Yield / %	Grade / wt%		Recovery / %	
		S	As	S	As
Pyrite concentrate	32.88	53.46	0.61	63.97	9.70
Middling I	7.46	44.46	2.08	12.08	7.51
Middling II	9.30	25.31	2.92	8.57	13.14
Tailing	50.35	8.40	2.86	15.39	69.65
Feed	100.00	27.48	2.07	100.00	100.00

**Fig. 5. Photograph of contact angle of pyrite and arsenopyrite after treating with different conditions.**

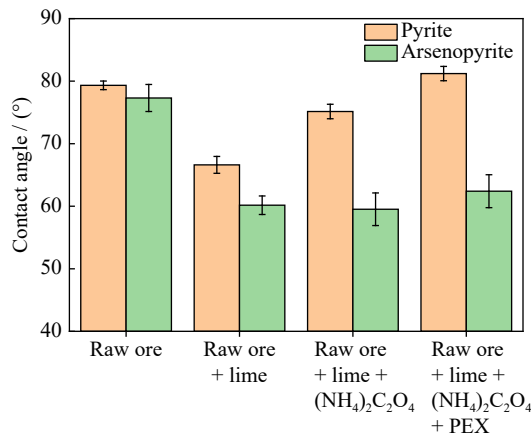


Fig. 6. Contact angle of pyrite and arsenopyrite under different reagents treatment.

3.3. Adsorption capacity test

The sulfide mineral floatability of the xanthate-induced flotation system mainly depends on the adsorption capacity of xanthate on the mineral surface [15–16]. Therefore, the effect of ammonium oxalate on the adsorption of PEX on the surface of pyrite and arsenopyrite in the lime system largely determines the flotation separation of pyrite and arsenopyrite. Therefore, the amount of PEX absorbed by pyrite and arsenopyrite at different activator concentrations was measured, and the results were presented in Fig. 7. The surface adsorption measurements were performed at 1×10^{-4} mol/L PEX and pH value of 11.

Without the addition of ammonium oxalate, the adsorption amounts of xanthate on the surface of pyrite and arsenopyrite maintained a low level. When the concentration of ammonium oxalate increased from 0 to 5×10^{-3} mol/L, the adsorption amounts of xanthate at the surface of pyrite and arsenopyrite increased from 1.20×10^{-7} to 1.79×10^{-6} mol/g and from 4.67×10^{-8} to 2.07×10^{-7} mol/g, respectively. Moreover, this further confirmed that ammonium oxalate

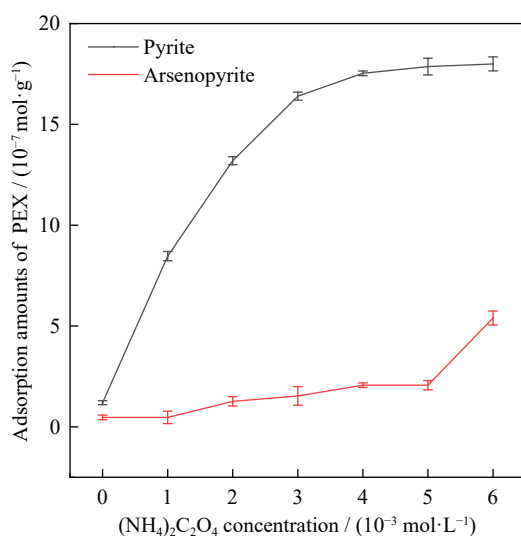


Fig. 7. Amounts of ethyl xanthate adsorbed on the pyrite and arsenopyrite surfaces as a function of the ammonium oxalate concentration.

could selectively activate pyrite and significantly increase the floatability difference between pyrite and arsenopyrite particles. These results are consistent with flotation tests and contact angle measurements.

3.4. Zeta potential analysis

The electrical double layer determines the adsorption of flotation reagents on the minerals–water interface. Zeta potential measurements can be used to test the electro-kinetic changes in different flotation reagent systems [17–18]. Fig. 8 showed the pyrite and arsenopyrite's zeta potential treated or untreated with PEX as a function of ammonium oxalate concentration in the lime system.

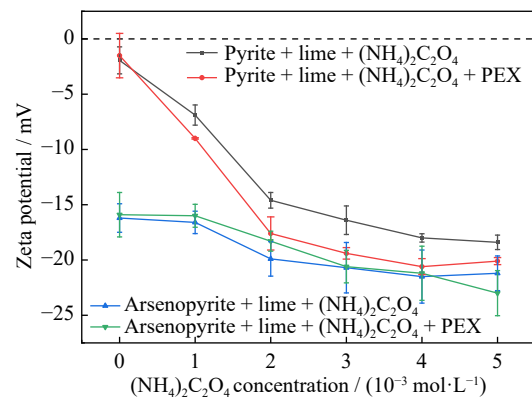


Fig. 8. Zeta potential of pyrite and arsenopyrite versus ammonium oxalate concentration in both KCl solution and calcium-rich supernatant treated or untreated with PEX.

Pyrite is expected to have a negative surface charge in alkaline conditions. However, under high alkalinity and high Ca^{2+} concentration, many hydrophilic CaOH^+ species and Ca^{2+} are adsorbed onto the negatively charged pyrite surface, resulting in a significant increase in the zeta potential on the pyrite surface [4,19–20]. As shown in Fig. 8, when ammonium oxalate was not added to the pulp, the surface potential of pyrite closed to zero, and when the collector was added, the zeta potential did not change, indicating that the surface of pyrite in the high alkaline and high calcium system could not adsorb PEX. With the addition of ammonium oxalate, the surface potential of pyrite decreased dramatically, illustrating that ammonium oxalate can effectively remove Ca^{2+} and its hydroxyl compounds on the surface of pyrite. After the activation of ammonium oxalate, continue to add PEX, the surface potential of pyrite was further decreased, indicating that the collector can be effectively adsorbed on the surface of activated pyrite.

However, the electronegative character of arsenopyrite decreased slightly after the addition of ammonium oxalate, indicating that the activation characteristic of ammonium oxalate on arsenopyrite was weak. Furthermore, the zeta potential of arsenopyrite showed no apparent change before and after interacting with PEX over the entire test concentration range, illustrating that PEX was hardly adsorbed on arsenopyrite surfaces. This result further proves that ammonium oxalate can selectively activate pyrite from arsenopyrite in

high alkalinity and high Ca^{2+} concentration system.

3.5. XPS analysis

The changes in the elemental content and surface properties of pyrite and arsenopyrite in the lime system before and after being activated by ammonium oxalate in the lime system were analyzed by XPS. The survey scan XPS spectra measured the atomic concentrations of C 1s, O 1s, S 2p, Ca 2p, Fe 2p, and As 3d (arsenopyrite samples). Simultaneously, the pyrite and arsenopyrite surface's element composition and binding energy before and after the activation of ammonium oxalate were investigated by the high-resolution XPS spectra. Therefore, these analyses can further explore the mechanism of ammonium oxalate on the pyrite and arsenopyrite's surface.

The XPS peak intensity integration method determined the surface atomic concentration of pyrite and arsenopyrite before and after interaction with ammonium oxalate in lime system, as shown in Fig. 9 and Table 4. Compared with pyrite treated with lime, the atomic concentration of S increased from 14.01% to 27.26%, and the atomic concentration of O decreased from 44.03% to 26.18% after 4×10^{-3} mol/L ammonium oxalate treatment, and the atomic concentration of

Ca on the surface of pyrite was removed. In contrast, the relative contents of S and O on the surface of arsenopyrite did not change significantly before and after the action of ammonium oxalate. This observation suggests that both pyrite and arsenopyrite produced hydrophilic surfaces in the lime system. The addition of ammonium oxalate can selectively remove the hydrophilic hydroxide and oxide on the surface of pyrite but has no noticeable effect on the hydrophilic film on the surface of arsenopyrite.

To further investigate surface chemical species formation on pyrite and arsenopyrite before and after the action of ammonium oxalate, the Multi-Pak software (version 9.3.0.3) was used for the peak fitting and separation of O 1s, S 2p, Fe 2p, and As 3d (arsenopyrite samples only) peaks in the high-resolution XPS spectra, and the binding energies and the relative contents on pyrite and arsenopyrite surface before and after ammonium oxalate treatment were analyzed. Figs. 10 and 11 and Tables 5 and 6 present the spectral peak deconvolution results and the corresponding data, respectively.

Fig. 10 shows the fitted peaks for high-resolution spectra of O 1s, S 2p, and Fe 2p of pyrite before and after ammonium oxalate treatment in the lime system. The semi-quantitative results of peak fitting parameters and elements are shown

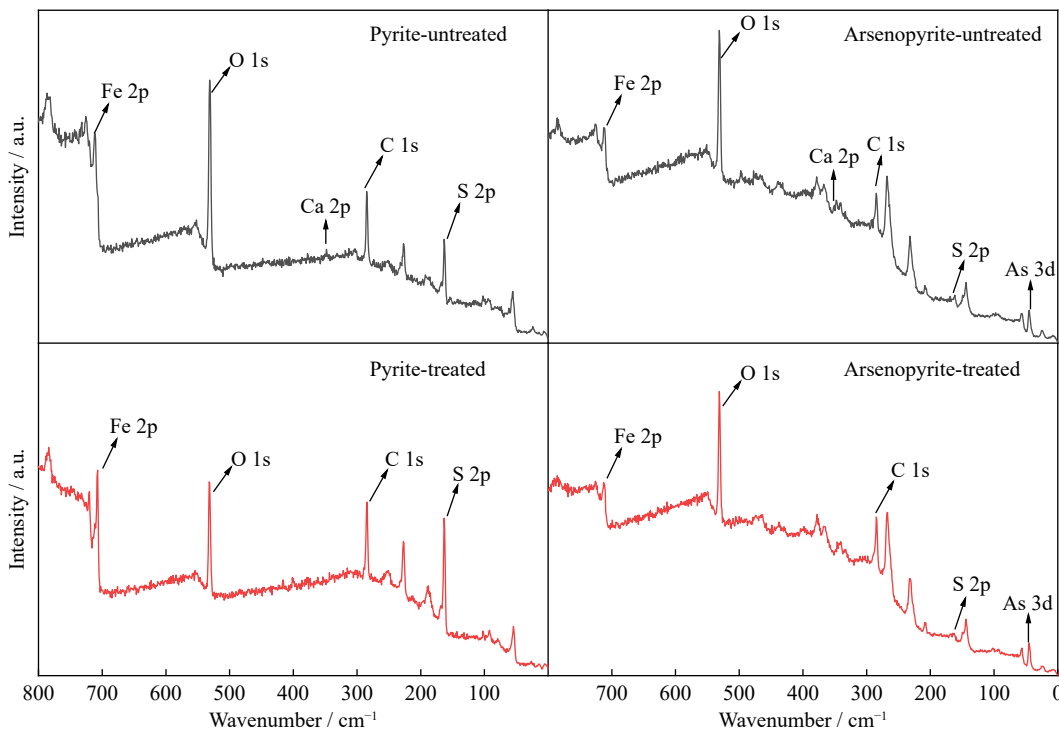


Fig. 9. Comprehensive XPS spectra of pyrite and arsenopyrite before and after ammonium oxalate treatment in the lime system.

Table 4. Atomic concentration of pyrite and arsenopyrite with and without the addition of 4×10^{-3} mol/L ammonium oxalate in the lime system

Sample	Atomic concentration / %					
	C 1s	O 1s	S 2p	Ca 2p	Fe 2p	As 3d
Pyrite-untreated	37.70	44.03	14.01	0.50	3.76	—
Pyrite-treated	39.14	26.18	27.26	—	7.42	—
Arsenopyrite-untreated	32.75	45.47	4.18	1.48	8.20	7.92
Arsenopyrite-treated	42.23	39.96	4.29	—	5.49	8.03

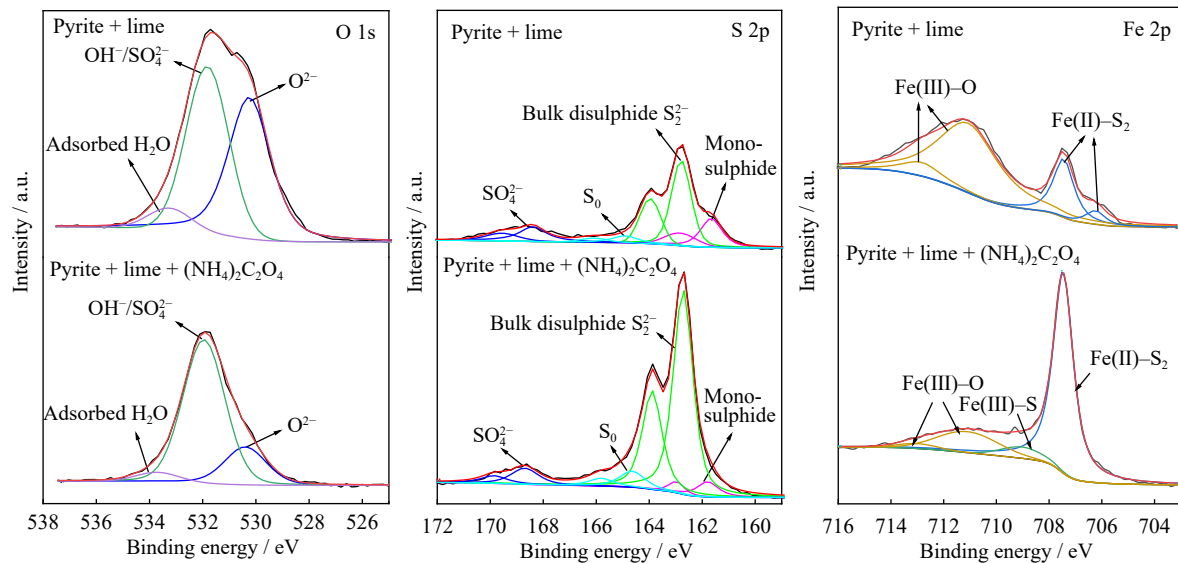


Fig. 10. O 1s, S 2p, and Fe 2p XPS spectra of pyrite with and without the addition of ammonium oxalate in the lime system.

in Table 5.

The O 1s spectra of the pyrite were composed of three characteristic peaks, the peak at (530.0 ± 0.1) eV corresponding to O^{2-} from FeO, Fe_2O_3 , CaO, and Fe_3O_4 [21–22]. The presence of Fe(III)–O peak in the Fe 2p spectrum and the presence of SO_4^{2-} in the S 2p spectrum suggest the possible hydroxide and sulfate phases at (531.9 ± 0.1) eV [23–27]. The binding energy at (533.5 ± 0.3) eV is attributed to adsorbed water [28]. After ammonium oxalate treatment, the relative content of O^{2-} on the surface of pyrite decreased from 47.61% to 20.72%, indicating that the hydrophilic oxide layer formed by the action of highly alkaline lime on the surface of pyrite has been effectively cleaned.

The S 2p spectra of the pyrite were composed of four components. Each component corresponded to a pair of S $2p_{3/2}$ and S $2p_{1/2}$ peaks. The S $2p_{3/2}$ component occurring at binding energies of 161.62 and 161.82 eV are attributable to the mono-sulfide (S^{2-}) species [29]. Similarly, the peaks occurring at 162.76 eV is attributable to the disulfide (S_2^{2-}) species [30]. The elemental sulfur (S_0) species formed on the pyrite surface occur at 164.70–164.90 eV, and the sulphate (SO_4^{2-}) species was found at the higher binding energy of 168 eV [31]. In the lime system, the sum of S_0 and SO_4^{2-} species was 24.18%, revealing that oxidation had occurred on the surface of pyrite, which reduces the xanthate-induced floatability of pyrite. After the action of ammonium oxalate, the sulphate content on the surface of pyrite decreased evidently, and the content of bulk disulfide S_2^{2-} species increased from 53.26% to 76.32%, indicating that the oxidation degree of pyrite treated with ammonium oxalate decreased significantly, and the original hydrophobic surface of sulfide ore was exposed.

For Fe 2p spectra of pyrite, the prominent peak near 706.2 and 707.4 eV were assigned to Fe(II)– S_2 , and the peak at 709.05 eV representing Fe(III)–S [25,31–32]. Peaks located at the high binding energy (711 and 713 eV) represent extensive oxidized iron products such as FeOOH and Fe_2O_3 [33–34]. On the surface of pyrite treated with lime, at least

75% of Fe exists as iron oxide or iron hydroxide, reflecting the nature that the Fe site in pyrite is easy to oxidize. In the lime system, pyrite activated by ammonium oxalate exposed a large number of fresh surfaces. The oxidized iron decreased to less than 20%, and the content of Fe(II)– S_2 in bulk pyrite increased to 74.27%. The results show that the addition of ammonium oxalate desorbs the hydrophilic compounds containing iron covered on the surface of pyrite. A new hydrophobic surface is formed on the mineral surface.

Fig. 11 shows the high-resolution XPS spectra and the spectral peak deconvolution results of O 1s, S 2p, Fe 2p, and As 3d on the arsenopyrite's surface with and without the addition of ammonium oxalate, and Table 6 presents the corresponding data of semi-quantitative results of peak fitting parameters and elements. For O 1s spectra of arsenopyrite, the prominent peak was best fitted with three components near 530.0, 531.2, and 532.6 eV, corresponding to O^{2-} , OH^-/SO_4^{2-} , and adsorbed water, respectively [21–24]. The S $2p_{3/2}$ component occurring at binding energies of (161.9 ± 0.1) eV is attributable to the mono-sulfide species [35]. Similarly, the peaks occurring at (163.9 ± 0.1) and (168.0 ± 0.1) eV are attributable to the polysulfide (S_n^{2-}) and sulphate (SO_4^{2-}), respectively [36]. The binding energies of Fe $2p_{3/2}$ spectra near 707.4, 711.0, and 712.7 eV correspond to the Fe(II) of FeAsS, Fe(III)–AsS, and Fe(III)–OH species, respectively [36–38]. The intense peak at (41.5 ± 0.1) eV belongs to As(–1) in arsenopyrite [39]. Additional peaks at binding energies of (43.8 ± 0.1) and (45.3 ± 0.1) eV were probably from As(III)–O and As(V)–O species [38–40].

Compared with before and after the action of ammonium oxalate, the species composition of O and Fe on the surface of arsenopyrite changed very slightly, and the Fe on arsenopyrite's surface was still Fe(III). Incredibly, S on the surface of arsenopyrite was further oxidized after the action of ammonium oxalate. The content of polysulfide (S_n^{2-}) increased from 17.36% to 28.73%, and the content of sulphate (SO_4^{2-}) increased from 24.37% to 28.04%. Meanwhile, As on the arsenopyrite's surface was further oxidized, and the con-

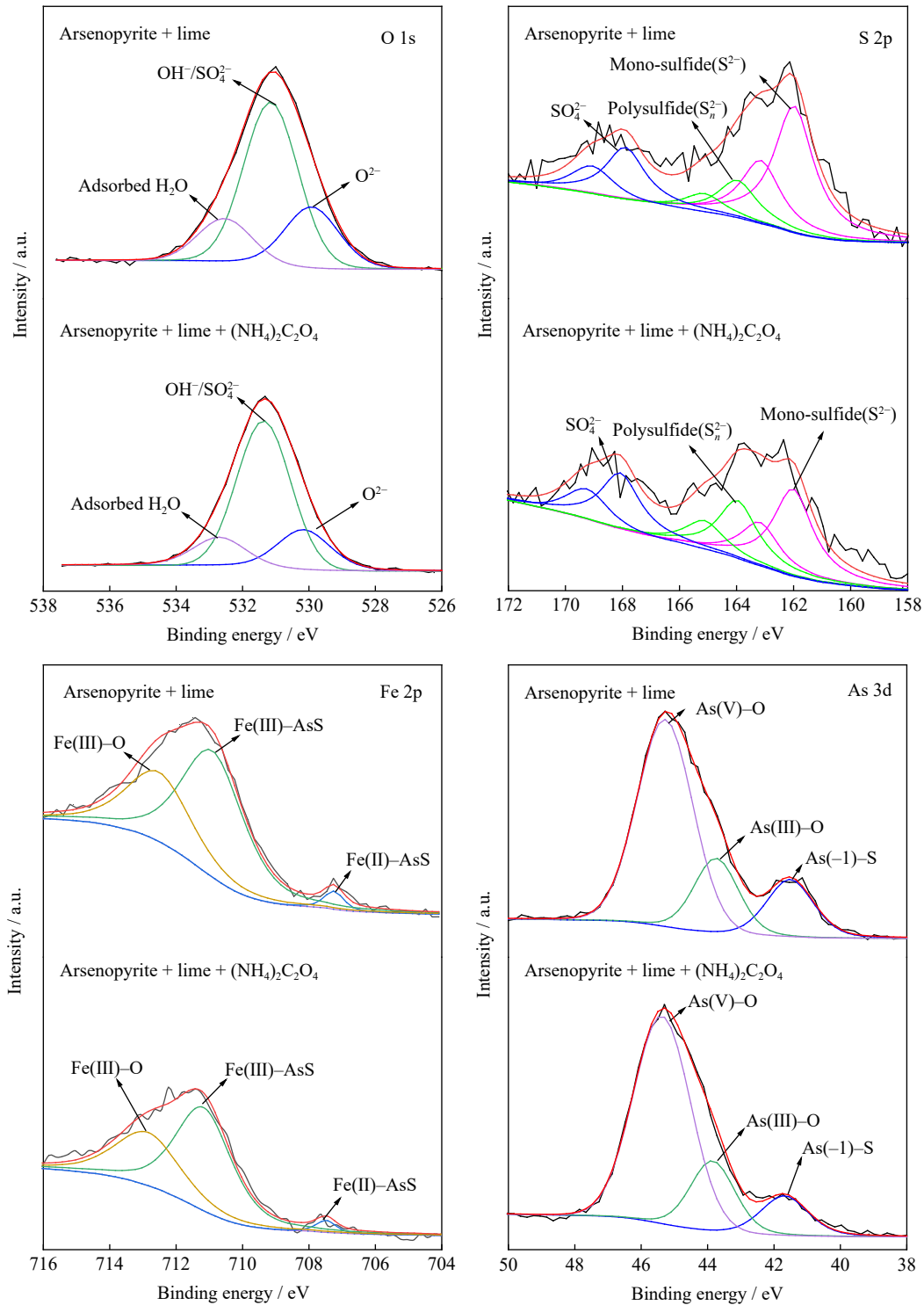


Fig. 11. O 1s, S 2p, Fe 2p, and As 3d XPS spectra of arsenopyrite with and without the addition of ammonium oxalate in the lime system.

tent of As(V) increased from 63.81% to 68.14%. This part of As(V) is mainly iron arsenate. The iron arsenate and iron oxide formed after the oxidation of arsenopyrite surface undergo ligand exchange in the mode of bidentate binuclear inner-sphere complex [41–42]. This structure is very stable on the surface of arsenopyrite and is difficult to interact with ammonium oxalate. The results show that adding ammonium oxalate did not clean the hydrophilic oxide film on the arsenopyrite surface and further increased the oxidation degree of the arsenopyrite surface. The XPS results showed that the ad-

dition of ammonium oxalate could selectively remove the hydrophilic and stable oxide film on the surface of pyrite in the lime system. The XPS analysis further confirmed the previous results of the flotation test, contact angle analysis, surface adsorption measurements analysis, and zeta potential analysis.

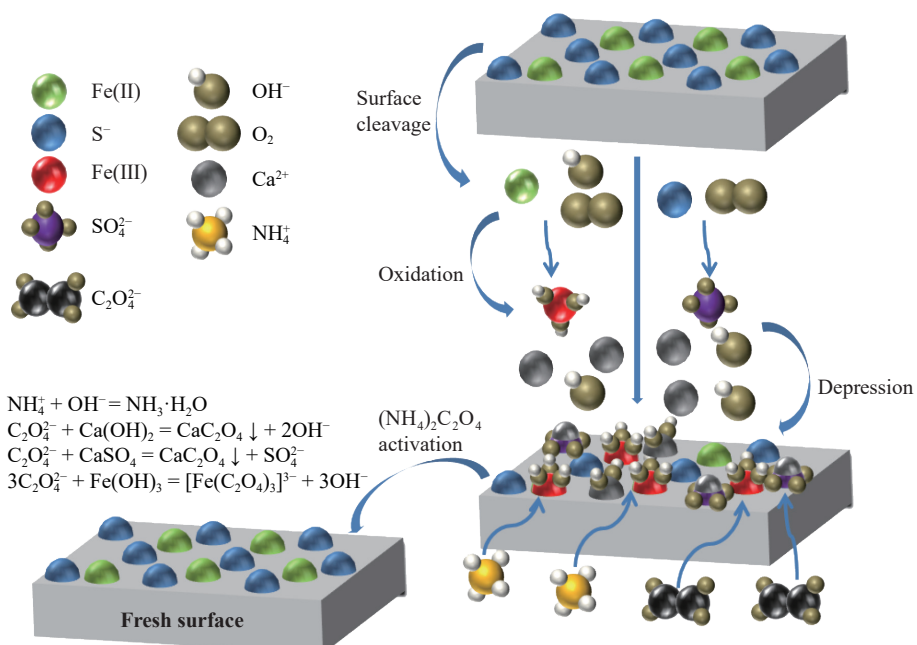
Based on the above data analysis results, a model is proposed to explain the selective activation of pyrite by adding (NH₄)₂C₂O₄ in the lime system during the pyrite–arsenopyrite flotation separation process (Fig. 12).

Table 5. Peak fit parameters (binding energies (BE), full peak width at half maximum (FWHM), and peak areas) of O 1s, S 2p, and Fe 2p on the pyrite surfaces

Peaks	Pyrite + lime			Pyrite + lime + ((NH ₄) ₂ C ₂ O ₄)		
	BE / eV	FWHM / eV	Area fraction / %	BE / eV	FWHM / eV	Area fraction / %
O 1s	530.24	1.88	47.61	530.38	1.88	20.72
	531.82	1.88	46.58	531.96	1.88	74.73
	533.25	1.88	5.81	533.75	1.88	4.55
S 2p	161.62	0.97	22.56	161.82	0.97	6.85
	162.76	0.88	53.26	162.76	0.88	76.32
	164.90	1.15	7.14	164.70	1.15	8.16
	168.42	1.24	17.04	168.78	1.24	8.67
Fe 2p	706.21	0.90	4.41	709.05	1.90	6.26
	707.43	0.93	19.71	707.46	0.93	74.27
	711.10	2.75	67.08	711.15	2.75	16.89
	712.89	1.80	8.79	713.08	1.80	2.58

Table 6. Peak fit parameters (binding energies (BE), full peak width at half maximum (FWHM), and peak areas) of O 1s, S 2p, Fe 2p, and As 3d on the arsenopyrite surfaces

Peaks	Arsenopyrite + lime			Arsenopyrite + lime + ((NH ₄) ₂ C ₂ O ₄)		
	BE / eV	FWHM / eV	Area fraction / %	BE / eV	FWHM / eV	Area fraction / %
O 1s	529.92	1.92	23.64	530.06	1.92	20.18
	531.15	1.92	60.28	531.27	1.92	65.20
	532.54	1.92	16.08	532.62	1.92	14.62
S 2p	161.94	1.70	58.27	161.90	1.70	43.23
	163.94	1.70	17.36	163.86	1.70	28.73
	167.93	1.70	24.37	168.03	1.70	28.04
Fe 2p	707.27	0.71	2.83	707.49	0.71	2.48
	710.96	2.23	61.46	711.17	2.00	60.70
	712.60	2.31	35.71	712.87	2.31	36.82
As 3d	41.46	1.70	16.65	41.57	1.70	12.36
	43.73	1.60	19.54	43.76	1.60	19.50
	45.29	2.01	63.81	45.31	2.06	68.14

**Fig. 12. Diagram showing the activation of pyrite by ammonium oxalate.**

4. Conclusions

In this work, ammonium oxalate was used in the flotation separation of pyrite and arsenopyrite separation in the lime system. The interaction mechanism between ammonium oxalate and pyrite or arsenopyrite was analyzed by the contact angle, adsorption experiments, zeta potential measurements, and XPS analysis. The following conclusions are obtained.

(1) All flotation experiments revealed that pyrite could be selectively separated from arsenopyrite in the lime system with ammonium oxalate as the activator.

(2) The pyrite's PEX adsorption capacity and zeta potential change were much greater than arsenopyrite after ammonium oxalate treatment in the lime system.

(3) The contact angle analysis and XPS analysis results show apparent differences in the oxidation products on the surface of pyrite and arsenopyrite in the lime system and the arsenate on the surface of arsenopyrite is difficult to remove by ammonium oxalate effectively. In contrast, the hydrophilic oxide film formed on the surface of pyrite is effectively cleaned by ammonium oxalate.

In summary, a novel activator for flotation separation of pyrite from arsenopyrite in the lime system was developed in this study.

Acknowledgements

This work was financially supported by Yunnan Major Scientific and Technological Projects, China (No. 202202AG050015), and National Natural Science Foundation of China (No. 51504109).

Conflict of Interest

The authors declare that they have no known competing financial interests or personal relationships that could have appeared to influence the work reported in this paper.

References

- [1] B. Fletcher, W. Chimonyo, and Y.J. Peng, A comparison of native starch, oxidized starch and CMC as copper-activated pyrite depressants, *Miner. Eng.*, 156(2020), art. No. 106532.
- [2] X.F. Zheng, S.T. Cao, Z.Y. Nie, et al., Impact of mechanical activation on bioleaching of pyrite: A DFT study, *Miner. Eng.*, 148(2020), art. No. 106209.
- [3] P.M. Ferreira, D. Majuste, E.T.F. Freitas, et al., Galvanic effect of pyrite on arsenic release from arsenopyrite dissolution in oxygen-depleted and oxygen-saturated circumneutral solutions, *J. Hazard. Mater.*, 412(2021), art. No. 125236.
- [4] M. Zanin, H. Lambert, and C.A. du Plessis, Lime use and functionality in sulphide mineral flotation: A review, *Miner. Eng.*, 143(2019), art. No. 105922.
- [5] X.H. Wang and K.S. Eric Forssberg, Mechanisms of pyrite flotation with xanthates, *Int. J. Miner. Process.*, 33(1991), No. 1-4, p. 275.
- [6] A.S. Stepanov, R.R. Large, E.S. Kiseeva, et al., Phase relations of arsenian pyrite and arsenopyrite, *Ore Geol. Rev.*, 136(2021), art. No. 104285.
- [7] A.M. Buswell, D.J. Bradshaw, P.J. Harris, and Z. Ekmekci, The use of electrochemical measurements in the flotation of a platinum group minerals (PGM) bearing ore, *Miner. Eng.*, 15(2002), No. 6, p. 395.
- [8] Y.H. Hu, S.L. Zhang, and G.Z. Qiu, Surface chemistry of activation of lime-depressed pyrite in flotation, *Trans. Nonferrous Met. Soc. China*, 10(2000), No. 6, p. 798.
- [9] S. Dzhamyarov, I. Grigorova, M. Ranchev, and I. Nishkov, Ammoniacal activation of lime depressed pyritea, [in] *Proc. of XXIX International Mineral Processing Congress*, Moscow, 2018.
- [10] R. Murphy and D.R. Strongin, Surface reactivity of pyrite and related sulfides, *Surf. Sci. Rep.*, 64(2009), No. 1, p. 1.
- [11] O. Kenji, T. Tsunehiko, and S. Kozo, Effect on some ammonium salts on the flotation of iron sulphide minerals, *Science Reports of the Research Institutes, Tohoku University. Ser. A, Physics, Chemistry and Metallurgy*, 12(1960), p. 62.
- [12] X. Xiaojun and Ş. Kelebek, Activation of xanthate flotation of pyrite by ammonium salts following its depression by lime, *Dev. Miner. Process.*, 13(2000), p. C8b.
- [13] Q. Zhang, S.M. Wen, Q.C. Feng, and H. Wang, Enhanced sulfidization of azurite surfaces by ammonium phosphate and its effect on flotation, *Int. J. Miner. Metall. Mater.*, 29(2022), No. 6, p. 1150.
- [14] X. Chen, G.H. Gu, and Z.X. Chen, Seaweed glue as a novel polymer depressant for the selective separation of chalcopyrite and galena, *Int. J. Miner. Metall. Mater.*, 26(2019), No. 12, p. 1495.
- [15] C. Han, D.Z. Wei, S.L. Gao, et al., Adsorption and desorption of butyl xanthate on chalcopyrite, *J. Mater. Res. Technol.*, 9(2020), No. 6, p. 12654.
- [16] S.A. Khoso, Y.H. Hu, F. Lü, et al., Xanthate interaction and flotation separation of H₂O₂-treated chalcopyrite and pyrite, *Trans. Nonferrous Met. Soc. China*, 29(2019), No. 12, p. 2604.
- [17] Y.F. Fu, W.Z. Yin, X.S. Dong, et al., New insights into the flotation responses of brucite and serpentine for different conditioning times: Surface dissolution behavior, *Int. J. Miner. Metall. Mater.*, 28(2021), No. 12, p. 1898.
- [18] W.J. Zhao, M.L. Wang, B. Yang, Q.C. Feng, and D.W. Liu, Enhanced sulfidization flotation mechanism of smithsonite in the synergistic activation system of copper-ammonium species, *Miner. Eng.*, 187(2022), art. No. 107796.
- [19] S.R. Rao and J.A. Finch, A review of water re-use in flotation, *Miner. Eng.*, 2(1989), No. 1, p. 65.
- [20] R.S. Multani, H. Williams, B. Johnson, R.H. Li, and K.E. Waters, The effect of superstructure on the zeta potential, xanthate adsorption, and flotation response of pyrrhotite, *Colloids Surf. A Physicochem. Eng. Aspects*, 551(2018), p. 108.
- [21] P. Galicia, N. Batina, and I. González, The relationship between the surface composition and electrical properties of corrosion films formed on carbon steel in alkaline sour medium: An XPS and EIS study, *J. Phys. Chem. B*, 110(2006), No. 29, p. 14398.
- [22] A.P. Grosvenor, B.A. Kobe, and N.S. McIntyre, Studies of the oxidation of iron by water vapour using X-ray photoelectron spectroscopy and QUASES™, *Surf. Sci.*, 572(2004), No. 2-3, p. 217.
- [23] C.F. Jones, S. LeCount, R.S.C. Smart, and T.J. White, Compositional and structural alteration of pyrrhotite surfaces in solution: XPS and XRD studies, *Appl. Surf. Sci.*, 55(1992), No. 1, p. 65.
- [24] N.S. McIntyre and D.G. Zetaruk, X-ray photoelectron spectroscopic studies of iron oxides, *Anal. Chem.*, 49(1977), No. 11, p. 1521.
- [25] H. Chen, Z.L. Zhang, Z.L. Yang, et al., Heterogeneous fenton-like catalytic degradation of 2, 4-dichlorophenoxyacetic acid in water with FeS, *Chem. Eng. J.*, 273(2015), p. 481.
- [26] M. Kartal, F. Xia, D. Ralph, et al., Enhancing chalcopyrite

- leaching by tetrachloroethylene-assisted removal of sulphur passivation and the mechanism of jarosite formation, *Hydrometallurgy*, 191(2020), art. No. 105192.
- [27] B. Feng, L.Z. Zhang, W.P. Zhang, H.H. Wang, and Z.Y. Gao, Mechanism of calcium lignosulfonate in apatite and dolomite flotation system, *Int. J. Miner. Metall. Mater.*, 29(2022), No. 9, p. 1697.
- [28] P. Li, J.Y. Lin, K.L. Tan, and J.Y. Lee, Electrochemical impedance and X-ray photoelectron spectroscopic studies of the inhibition of mild steel corrosion in acids by cyclohexylamine, *Electrochim. Acta*, 42(1997), No. 4, p. 605.
- [29] R.S.C. Smart, W.M. Skinner, and A.R. Gerson, XPS of sulphide mineral surfaces: Metal-deficient, polysulphides, defects and elemental sulphur, *Surf. Interface Anal.*, 28(1999), No. 1, p. 101.
- [30] R.P. Liao, Q.C. Feng, S.M. Wen, and J. Liu, Flotation separation of molybdenite from chalcopyrite using ferrate(VI) as selective depressant in the absence of a collector, *Miner. Eng.*, 152(2020), art. No. 106369.
- [31] M. Mullet, S. Boursiquot, M. Abdelmoula, J.M. Génin, and J.J. Ehrhardt, Surface chemistry and structural properties of mackinawite prepared by reaction of sulfide ions with metallic iron, *Geochim. Cosmochim. Acta*, 66(2002), No. 5, p. 829.
- [32] H.W. Nesbitt, G.M. Bancroft, A.R. Pratt, and M.J. Scaini, Sulphur and iron surface states on fractured pyrite surfaces, *Am. Mineral.*, 83(1998), No. 9-10, p. 1067.
- [33] P. Forson, M. Zanin, W. Skinner, and R. Asamoah, Differential flotation of pyrite and arsenopyrite: Effect of hydrogen peroxide and collector type, *Miner. Eng.*, 163(2021), art. No. 106808.
- [34] H. Gholami, B. Rezai, A. Hassanzadeh, A. Mehdilo, and M. Yarahmadi, Effect of microwave pretreatment on grinding and flotation kinetics of copper complex ore, *Int. J. Miner. Metall. Mater.*, 28(2021), No. 12, p. 1887.
- [35] Y.L. Mikhlin, A.S. Romanchenko, and I.P. Asanov, Oxidation of arsenopyrite and deposition of gold on the oxidized surfaces: A scanning probe microscopy, tunneling spectroscopy and XPS study, *Geochim. Cosmochim. Acta*, 70(2006), No. 19, p. 4874.
- [36] C.L. Corkhill, P.L. Wincott, J.R. Lloyd, and D.J. Vaughan, The oxidative dissolution of arsenopyrite (FeAsS) and enargite (Cu₃AsS₄) by leptospirillum ferrooxidans, *Geochim. Cosmochim. Acta*, 72(2008), No. 23, p. 5616.
- [37] H.W. Nesbitt, I.J. Muir, and A.R. Prarr, Oxidation of arsenopyrite by air and air-saturated, distilled water, and implications for mechanism of oxidation, *Geochim. Cosmochim. Acta*, 59(1995), No. 9, p. 1773.
- [38] H.W. Nesbitt and I.J. Muir, Oxidation states and speciation of secondary products on pyrite and arsenopyrite reacted with mine waste waters and air, *Mineral. Petrol.*, 62(1998), No. 1-2, p. 123.
- [39] M.C. Costa, A.M. Botelho do Rego, and L.M. Abrantes, Characterization of a natural and an electro-oxidized arsenopyrite: A study on electrochemical and X-ray photoelectron spectroscopy, *Int. J. Miner. Process.*, 65(2002), No. 2, p. 83.
- [40] F.J. Grunthaner, P.J. Grunthaner, R.P. Vasquez, B.F. Lewis, J. Maserjian, and A. Madhukar, Local atomic and electronic structure of oxide/GaAs and SiO₂/Si interfaces using high-resolution XPS, *J. Vac. Sci. Technol.*, 16(1979), No. 5, p. 1443.
- [41] Y. Du, Q. Lu, H.Y. Chen, Y.G. Du, and D.Y. Du, A novel strategy for arsenic removal from dirty acid wastewater via CaCO₃-Ca(OH)₂-Fe(III) processing, *J. Water Process. Eng.*, 12(2016), p. 41.
- [42] Y.F. Jia, L.Y. Xu, X. Wang, and G.P. Demopoulos, Infrared spectroscopic and X-ray diffraction characterization of the nature of adsorbed arsenate on ferrihydrite, *Geochim. Cosmochim. Acta*, 71(2007), No. 7, p. 1643.